Journal Pre-proof

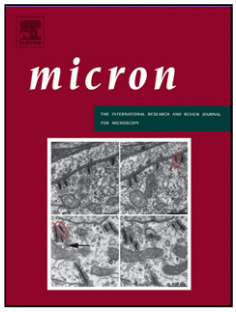

3D-printed multisampling holder for microcomputed tomography applied to life and materials science research

Isabel Vasconcelos, Margarida Franco, Mário Pereira, Isabel Duarte, António Ginjeira, Nuno Alves

PII: S0968-4328(21)00133-5

DOI: https://doi.org/10.1016/j.micron.2021.103142

Reference: JMIC 103142

To appear in: *Micron*

Received Date: 2 April 2021

Revised Date: 15 August 2021

Accepted Date: 22 August 2021

Please cite this article as: Vasconcelos I, Franco M, Pereira M, Duarte I, Ginjeira A, Alves N, 3D-printed multisampling holder for microcomputed tomography applied to life and materials science research, *Micron* (2021), doi: https://doi.org/10.1016/j.micron.2021.103142

3D-printed multisampling holder for microcomputed tomography applied to life and materials science research

Isabel Vasconcelos[a,b,*]isabelvascon@hotmail.com, Margarida Franco[b], Mário Pereira[a,b], Isabel Duarte[c], António Ginjeira[a], Nuno Alves[b]

[a]Department of Endodontics Faculdade de Medicina Dentária Universidade de Lisboa, Lisbon, Portugal Rua Professora Teresa Ambrósio, Cidade Universitária, 1600-277, Lisboa, Portugal
[b]Center for Rapid and Sustainable Product Development Polytechnic Institute of Leiria, Portugal Rua de Portugal, 2430-028, Marinha Grande, Portugal
[c]Centre for Mechanical Technology and Automation Department of Mechanical Engineering University of Aveiro, 3810-193, Aveiro, Portugal
[*]Corresponding author at: Department of Endodontics Faculdade de Medicina Dentária da Universidade de Lisboa Rua Professora Teresa Ambrósio, Cidade Universitária, 1600-277, Lisboa, Portugal.

Highlights

- Microcomputed tomography is a nondestructive and noninvasive method applied in life science and material science.
- The classic solutions of sampling mounting show some limitations when the research includes a large number of samples.
- The 3D printing process enables the fabrication of a holder, which exactly fits the experimental setup.
- A multisampling holder gives the possibility to do multi-analysis at the same time, in the same scan, which dramatically reduces the scan duration time, cost and data storage, and consequently, reduces human and equipment resources.

Abstract

The aim of this work was to design, fabricate, test and validate a 3D-printed multisampling holder for multi-analysis by microcomputed tomography. Different raw materials were scanned by microcomputed tomography. The raw material chosen was used to fabricate the holder by 3D printing. To validate the multisampling holder, five teeth were filled with a high density-material and scanned in two ways: a single and a multisampling scan mode. For each tooth, the root canal filling volume, porosity volume, closed pore volume, and open pore volume were calculated and compared when the same tooth was scanned in the two sampling scan mode. ABSplus P430™ allowed a high transmission value (84.3 %), and then it was the polymeric material selected to fabricate the holder. In a single sampling scan mode, the scan duration for scanning five teeth was 87.42 minutes, contrasting with 21.51 minutes for a multisampling scan mode, which scanned five teeth at the same time. The scan duration time and the cost using a multisampling holder represented a reduction of 75 % and the data

volume generated represented a reduction of 60 %. Comparing the two scan modes, the results also showed that the difference of root canal filling volume, porosity volume, closed pore volume, and open pore volume was not statistically significant ($p > .05$). The multisampling holder was validated to do multi-analysis by microcomputed tomography without significant loss of quantitative accuracy data, allowing a reduction in scan duration time, imaging cost, and data storage.

Keywords: 3-D printing, microcomputed tomography, multisampling holder

1. Introduction

The use of microcomputed tomography (micro-CT) has increased, and it has spread to multiple research fields, in life (Celikten *et al.*, 2016; Longo *et al.*, 2016; Sacco *et al.*, 2017; Zhang *et al.*, 2017) and material science (Ketcham and Carlson, 2001; Leszczyński *et al.*, 2016; Latief *et al.*, 2017). In different fields, the sample can be evaluated by micro-CT, with the advantage of being a nondestructive technique that preserves the sample analysed.

There is a variety of micro-CT scanner models. The SkyScan 1174 (Bruker, Kontich, Belgium) is a compact desktop micro-CT scanner in which the positions of the source, sample and camera are fixed. Variable magnification is achieved by the optical coupling between scintillator and charged coupled device (CCD) in the camera being provided by a variable magnification series of lenses. Thus the light output of the scintillator is conveyed to the CCD with variable magnification. This differs from many laboratory micro-CT systems, including the SkyScan 1275 (Bruker, Kontich, Belgium), in which magnification is changed by moving the sample between source and detector. The desktop SkyScan 1275 is a 3D X-ray model, designed for fast scanning of a wide range of samples. Thanks to the fast flat-panel detector the scanner is able to do faster scans. The X-ray source of this micro-CT model allows a range of kV between 20 to 100. The X-ray detector with active pixel CMOS flat-panel, with 3MP (1944 x 1536) contributes to optimize signal-to-noise ratio. However, in the SkyScan 1174 micro-CT model the maximum tube voltage is 50 kV. Independently of the micro-CT models, the principles are similar. They are based on an X-ray source, which produces the X-ray emission that passes through a turntable sample and is projected on a digital detector. The projection images are taken incrementally over a total rotation of either 180 º or 360 º. The acquired radiographs are mathematically reconstructed into slices allowing the reconstruction of three-dimensional (3D) volume (du Plessis *et al.*, 2017). The optimisation of all steps related to a micro-CT imaging is crucial to obtain the most reliable results. These steps include (i) sample preparation; (ii) sample mounting; (iii) kilovoltage, nominal

resolution, rotation, rotation step, frame averaging, flat-field correction, filter, which are scan parameters selected by the operator; (iv) reconstruction settings, like ring artifact correction, smoothing, beam hardening correction or attenuation coefficient range, also selected by the operator; (v) and thresholding, which consist in the selection of different values of threshold, made by the researcher.

Therefore, the first step in image acquisition involves preparation and positioning of the sample on the sample holder. Micro-CT requires very little, if any, sample preparation, and a sample can usually be scanned exactly as provided. Because of the rotating sample design of industrial micro-CT scanners, it is important to hold the sample correctly to avoid movement during scanning (Bouxsein *et al.*, 2010). While mounting a sample for micro-CT imaging, a golden rule is that, apart from the controlled rotation of the whole object during scanning, there must be no other movement of the object or any part of it to reduce the potential creation of artefacts (du Plessis *et al.*, 2017).

Related to sample mounting, two important aspects should be accomplished: (i) the holder material must be made by a non-attenuating material, presented a low attenuation coefficient and (ii) the efficacy of the immobilisation of the sample. Considering the holder material, the concept of partial absorption is fundamental. As the X-rays pass through the object being scanned, the signal is attenuated by scattering and absorption (Ketcham and Carlson, 2001). Thus, the filter and voltage settings are adjusted to obtain a transmission between 10 % and 50 % (aiming for 30 % to optimal conditions) to increase the signal to noise ratio (Bouxsein *et al.*, 2010). These parameters are usually adjusted for the highest density or worst angle of the sample to get the best possible transmission through the sample. Furthermore, the transmission of the X-rays through the holder should be taken into account to avoid any interference from the material holder. Materials that have a lower attenuation coefficient may be preferred (Cheng *et al.*, 2009). Low-density foam or other non-attenuating material is useful to position firmly the sample. Micro-CT users have been improvising micro-CT holders, e.g., plasticine (although this leaves a small residue on the sample), ‘parafilm’, plastic or expanded polystyrene tubes. Furthermore, all commercial available micro-CT systems supply to the users a variety of sample holders, but no one provides a possibility to hold and identify a variety of samples in a numbered position holder in the same scan. Imaging a large number of samples and serial scans increases the cost of imaging and also limits equipment and human resources available for other investigations. In addition, it generates large volume of data for storage and processing (Yagi *et al.*, 2014).

A solution that allows simultaneously multisampling scanning and multi-analysis on the same scan could be useful to reduce sources and time consumption. These two important aspects are in correlation: time consumption has a direct effect on human resources and a maximum number of samples that can be characterised within a reduced period of time will have a direct effect on the X-ray tube´s lifetime.

The limitations of the classic way for sample mounting could be overcome by specially designed holders, which exactly fit the experimental setup. The possibility to create individual appliances directly in the laboratory, by 3D printing within a reasonably short time constitutes an immense advantage. Additive manufacturing is a popular rapid prototyping process that can solve design problem and optimize the fabrication process. It is also named 3D printing (Khosravani and Reinicke, 2020). Different manufacturing processes have been developed. American Society for Testing Materials (ASTM) classified 3D printing techniques into seven categories: binder jetting, material extrusion, directed energy deposition, material jetting, sheet lamination, powder bed fusion, and vat photopolymerization. In relation to the 3D printers used in the present study, two additive manufacturing processes were used: material extrusion and material jetting. Material extrusion involves the heating of the raw material and molten material coming out of the nozzle. The part can be created layer by layer via movements of the nozzle. Thermoplastic materials are used in material extrusion to print the components. Fused deposition modeling (FDM) is an example of this 3D printing process (Khosravani and Reinicke, 2020). Material jetting is an accurate 3D printing technology, where firstly the raw material should be heated to reach the desired viscosity. Then, print heads moves and begin printing. The ultraviolet light source can cure the sprayed photopolymer resin. This process should be repeated until last layer of the part (Khosravani and Reinicke, 2020). Therefore, the 3D printing technologies enable direct manufacturing of functional, detailed and complex prototypes in a fast and efficient way (Herrmann *et al*., 2014). The 3D printing can be applied to create a customised micro-CT sample holder, according to a specific need.

According to our knowledge, a device for micro-CT that allows the inclusion of several samples in the same scan with the possibility of identifying the different samples according to the numbers inserted into the holder during and after the scan is lacking. So, the aims of this work are:

- To look for a holder material, which enables the best possible X-ray transmission.
- To design and fabricate a holder for multisampling and multi-analysis by micro-CT.

- To validate the holder, comparing the root canal filling volume, porosity volume, closed pore volume, and open pore volume of a single tooth in a holder (single sampling scan mode) with the same tooth integrated in the holder with other teeth, scanned simultaneously (multisampling scan mode).
- To test the holder, comparing the scan duration time, the cost estimation, and the data storage between the single sampling scan mode and the multisampling scan mode.

2. Methods

2.1. Holder material selection

To look for the more appropriate non-attenuating X-ray material to fabricate the holder, eight different materials were tested: Dental Wax (Kerr™, Bioggio, Switzerland), a paraffin and hydrocarbon-based material; RGD 720 (STRATASYS, Rehovot, Israel), an arginylglycylaspartic acid-based material; Rigur™ RGD 450 (STRATASYS, Rehovot, Israel), an arginylglycylaspartic acid-based material; VeroClear™ (STRATASYS, Rehovot, Israel), that simulates polymethyl methacrylate, commonly known as acrylic; ABSplus™ P430 (STRATASYS, Rehovot, Israel), an acrylonitrile butadiene styrene-based material; ABS Black (PrimaValue, Malmo, Sweden), an acrylonitrile butadiene styrene-based material; PLA (BQ, Madrid, Spain), a polylactic acid-based material; and PETG (RepRap, Cacém, Portugal), a polyethene terephthalate glycol copolyester-based material. The raw materials were 3D-printed with the same parallelepiped geometry (30 mm x 10 mm x 3.0 mm). Fig. 1 shows the 3D-printed raw materials tested and Table 1 summarises the 3D printer, slicer, raw materials, commercial materials, manufacturer, and technology associated in 3D printing process.

To test the micro-CT transmission of each raw material, the parallelepiped was positioned inside the chamber of the SkyScan 1174 micro-CT model (Bruker, Kontich, Belgium), according to the worst scenario orientation in terms of thickness. The scan parameters selected were pixel size 19.61 μm, X-ray tube voltage of 50 kV, X-ray intensity of 800 mA, exposure time of 6500 ms, rotation step of 0.9 º, and without aluminum filter. All of the assays were done in triplicate. The values of micro-CT transmission (%) through and above each raw material tested were registered. The micro-CT transmission (%) was reported as the minimum (Min) of transmission and average (Av), with and without flat-field (ff) correction.

2.2 Holder Design

The holder was designed with the use of a computer-aided design (CAD) software (Solidworks 2017, Dassault Systems, Massachusetts, USA), taking into account the dimensions of the brass tray base supplied by the manufacturer, with a diameter of 25 mm, which will be the support of the multisampling holder (Fig. 2). The geometry of the holder was a cylinder with a height of 6 mm and a maximum diameter of 35 mm with specific features (Fig. 3).

The bottom of the holder had a circular section with outer and inner diameters of 30 mm and 26 mm, respectively, and a height of 3 mm. The inner circular section aimed to externally fit the brass tray base supplied by manufacturer, to stabilise the holder.

At the base of the bottom (Fig. 4A) there were five numbers embossed (digits 1 to 5) to help the operator with placing the samples as well as recognizing them while reconstructing the projection images (Fig. 4B). The positions for each sample were equidistant from the centre of field of view (FOV), and designed to allow the simultaneous imaging of up to five teeth (or other types of specimens) within the same single FOV.

The upper part of the holder had a circular section with outer and inner diameters of 35 mm and 32 mm, respectively, and a height of 3 mm. In the lateral wall and also on the upper side, there were five numbers embossed (digits 1 to 5) following the same numbers embossed at the bottom side of the holder. This lateral numeration also could help the operator to recognise the known sequence of the samples.

The described geometry was exported as a standard tessellation languague (STL) file to the software Preform for Mac (Formlabs, Sommerville, MA, USA), in which the support structure required for printing was added, and the file was prepared for the 3D printing process with the previously selected raw material that enabled the best X-ray transmission.

2.3 Validation: effect of the single versus multisampling scan mode

To validate the holder, the root canal filling volume, total porosity volume, closed pore volume, and open pore volume were compared in two different scan modes. The methodology employed was to compare these dependent variables for the same tooth after performing two sampling positioning modes.

Five roots were selected, and the canals were shaped with Protaper Next system (Dentsply Maillefer, Ballaigues, Switzerland) until X4. Between each instrument, the canal was irrigated with 2 mL of a freshly prepared, 5.25 % sodium hypochlorite (NaOCl) solution (van der Sluis *et al.*, 2006) at 2 mm short of the working length (WL) (Boutsioukis *et al.*, 2010). A final irrigation protocol consisted of 2 mL of 5.25 % NaOCl passively activated for 1 min (20 s, three times) (van der Sluis *et al.*, 2010), with an ultrasonic tip ISO 20 25 mm (IrriSafe; Satelec, Acteon Group, Merignac Cedex, France) positioned at 1 mm short of WL (Jiang *et al.*, 2010). The smear layer was removed by 1 mL of 17 % EDTA for 1 min (Ozdemir *et al.*, 2012), followed by 2 mL of 5.25 % NaOCl. The canals were dried with absorbent X4 paper points (Dentsply Maillefer, Ballaigues, Switzerland). The root canal filling was performed using the continuous wave condensation technique, with a .08-tapered heat carrier of the B&L system (B&L Biotech, Seoul, Republic of Korea). The canals were filled using AH Plus JET sealer (Dentsply DeTrey GmbH, Konstanz, Germany), a resin epoxy-based sealer. The sealer was placed in the Protaper X4 gutta-percha (trans-isomer of polyisoprene) cones tip (Dentsply Maillefer, Ballaigues, Switzerland).

After the root canal filling, the teeth were submitted to micro-CT analysis. First, the scanning was performed by a single sampling scan mode, with a tooth '1' positioned in the centre of the FOV, in a conventional holder, supplied by the manufacturer (Fig. 5A). The single scan mode was done for each of the five teeth. Then, the multisampling scan mode was performed with the same teeth used in a single scan mode (Fig. 5B). The tooth '1' was fitted in the position '1' of the holder but scanned simultaneously with other teeth placed in the positions '2' to '5'. The teeth were fitted in each numbered position with dental wax. The brass tray sample base, supplied by the manufacturer, with a diameter of 25 mm, was selected and positioned into the micro-CT internal camera. The base has a peripheral rim, which was used to sustain the constructed holder, with an inner diameter of 26 mm (Fig. 2). The constructed holder was stabilised over the brass tray sample base with dental wax.

In a single or multisampling scan mode, the teeth were mounted into the holder and positioned inside a micro-CT chamber. The micro-CT model used for the validation was SkyScan 1275 (Bruker, Kontich, Belgium). The scan parameters selected were pixel size 19.61 μm, X-ray tube voltage of 80 kV, X-ray intensity of 125 mA, exposure time of 58 ms, rotation step of 0.5 º, 360 º rotation, and frame averaging 3 and 1 mm aluminum filter. The acquired projection images were reconstructed into cross-sectional slices

using the NRecon v.1.7.3.1 software (Bruker, Kontich, Belgium). Before rendering, for the same tooth, the data sets from the single sampling scan mode and the data sets from multisampling scan mode were coregistered in DataViewer software (Bruker, Kontich, Belgium). Then, the root filling models were rendered with the CTAn v.1.17.7.2 software (Bruker, Kontich, Belgium) and the volume of the root canal filling, porosity volume, closed pore volume, and open pore volume were calculated for the single and multisampling scan mode.

2.4 Effect of single versus multisampling scan mode on scan duration time, cost estimation, and data storage

The scan duration time (minutes: seconds) was estimated for the five samples (teeth), scanned by a single sampling scan mode and by a multisampling san mode. To scan five teeth in a single sampling scan mode, five scans were needed. However, to scan five teeth in a multisampling scan mode, just one scan was needed, because the five teeth were scanned simultaneously, at the same scan.

For the imaging cost estimation were considered two factors: scanning cost estimation, which considered 'x' as a minor unit cost for micro-CT scanning, and the data storage, in gigabyte (GB). The cost was related to the charges in the institute where the micro-CT scans were done. Related to data storage a counting of the storage (GB) was done. Data volume included all files created and stored during the acquisition and reconstruction image.

2.5 Statistical Analysis

Statistical analysis was performed using SPSS® (IBM® SPSS® Statistics version 24.0, IBM, USA). A paired-sample t-test was used to determine whether there was a statistically significant difference between the root canal filling volume (mm^3), porosity filling volume (mm^3), closed pore volume (mm^3), and open pore volume (mm^3), when the same tooth was submitted to a single sampling scan mode and a multisampling scan mode. A confidence interval of the difference (CI) of 95 %, t-value (t), the degrees of freedom (df), and a statistical significance value (p-value or Sig. 2-tailed of the paired-samples t-test) at the level of 5 % ($p < .05$) were considered.

3. Results & discussion

3.1 Holder material selection

The sample mounting is an important step of the micro-CT process. However, the classic way (Fig. 5A) for sample mounting has limitations mainly when the research includes a large number of samples to be analysed. In this study, a multisampling holder was fabricated, validated and compared with the classic single sampling scan mode.

Regarding the X-ray transmission through the raw material tested, the values of micro-CT transmission are presented in Table 2. For each material tested, the value of X-ray transmission (average) was from the best to the worst transmission: ABS P430™, 84.3 %; ABS Black, 84.2 %; Dental Wax, 83.7 % RGD720, 82.1 %; VeroClear™, 81.8 %; Rigur™ RGD 450, 81.7 %; PLA, 81.6 %; and PETG, 81.1 %. ABSplus P430™ was the raw material selected to fabricate the holder, which allowed a high X-ray transmission value (84.3 %). The polymeric materials selection was dependent on the 3D printers used in the present study, since a specific 3D printer using a specific technology requires a specific raw material to be associated to the 3D printing process. Regarding the dental wax, used as raw material, it was already mentioned in the discussion section that the dental wax was tested because it is an easy and inexpensive material often used by the micro-CT users to 'glue' the sample onto the classic solution on sample mounting.

Then, the 3D-printed holder was fabricated and it was projected to fit inside the internal chamber of the micro-CT model used (SkyScan 1275), which is big enough to fit five molars at the same time (Fig. 5B). There are a variety of micro-CT models dedicated to material and life sciences. In the SkyScan 1275 model (Bruker, Kontich, Belgium) is possible to fit a holder with 96 mm diameter and 120 mm length. Furthermore, the multifunctional sampling holder can be designed with one, two or more platforms (Fig. 5C), adapting the number for positioning the samples, optimizing even more the micro-CT scan time. In this case is mandatory to decrease the nominal resolution to fit all the teeth or other kind of samples inside the FOV. The limitation of the number of platforms will be always related to the size of the sample analyzed, the nominal resolution needed, the FOV dimensions and the size of the internal chamber of micro-CT model used.

On the other hand, one of the limitations of this work was to select the 3D printing process to obtain the same shape and geometry of the raw material to test, to select the one that enables the best X-ray transmission. For each raw material tested, a specific 3D printing process was associated. Two of the processes often used in 3D printing are the extrusion-based (EB) process and material jetting (MJ). The EB process is often referred to as fused deposition modelling (FDM). MJ is also referred to as Polyjet™. FDM is most common, especially for private use as it is relatively inexpensive, although less accurate (Kim *et al.*, 2016). MJ printing devices are more precise but are more expensive (van Noort, 2012). It was not possible to standardise the 3D printing processes. In materials like ABS P430, ABS Black, PLA, and PETG, the process used was material extrusion. In the other raw materials (RGD 720, RGD 450, and VeroClear), the technology used was material jetting. The pattern and structure are dependent on the raw material but also related to printing conditions, e.g., nozzle size, deposition velocity and temperature (Branco *et al.*, 2020). This way, the manufactured samples could have different internal pattern, with different 'solid' printing, and thus different printing quality. Having air bubbles inside could show higher transmission. This way, the good X-ray transmission value could be related not only to the raw material but also to the presence of porosity. This could be overcome with the suggestion of a future work, to perform morphometric micro-CT analysis of the polymeric samples, to understand if there is a relationship between porosity and the transmission value. Then, a more reliable selection could be made for the best raw material to fabricate the holder.

3.2 Validation: effect of the single versus multisampling scan mode

Most micro-CT studies do not have any data about the use of a specific holder. In literature, just a few references regarding the use of a customised micro-CT holder can be found, but with no similar description of the device developed in this work. Some descriptions about holders are used by some authors: 'customised silicone or custom sample holder' (Angerame *et al.*, 2012; Alshehri *et al.*, 2016); 'the roots were fixed in a cylindrical container with foam' (Moeller *et al.*, 2013); 'the root-tip side of each specimen was embedded in self-curing acrylic resin; silicone tubes matching the external diameter of the acrylic stubs were fitted and filled with phosphate-buffered saline, to prevent dehydration of the roots during the scanning procedures in the CT' (Moinzadeh *et al.*, 2016); and simple solution like 'SEM stubs' (Rechenberg and

Paqué, 2013). Only two articles have a more detailed description closer to the multisampling holder described in this work: 'the teeth were individually embedded in high-precision impression material (Speedex; Coltène, Cuyahoga Falls, OH) with the access cavities facing down. Subsequently, groups of 7 teeth were positioned in a sample holder and were brought to the fiber carbon bed of the micro-CT scanner' (Freire *et al.*, 2015; Iglecias *et al.*, 2017).

However, according to our knowledge, none of the studies included a validation of a multisampling scan mode. So, this study was designed to validate data volumes comparing the two modes of sampling. The holder proposed with a numeration system allowed the identification of the samples duting the micro-CT process, and also the numbers inserted in the lateral wall of the holder helps to identify the samples due to the numbers at the upper side of the holder are covered when the teeth are positioned and stabilised with dental wax in each of the numbered position.

However, possible drawbacks of placing several samples simultaneously in a micro-CT scanner include increased signal attenuation and scatter related to an increased in object mass in FOV. To fit several samples in the same holder and then in the same scan, the samples have to be positioned away from the centre of the FOV, where the performance of the scanner is optimised. It could expect some loss of resolution and sensitivity, which could have a significant impact on the image quality and quantitative accuracy of the sample scanned off-centre, relative to those scanned near the centre of FOV of the scanner (Siepel *et al.*, 2010). In order to that it was fundamental to validate the data using a multisampling holder to understand if the outcome was significantly different when compared to a single sampling scan mode. The volume of the root canal filling, porosity filling, closed pore, and open pore was analyzed, and it was expected that the volume must be the same for both scan protocols, the single sampling scan mode and the multisampling scan mode.

The results regarding the two scan modes are presented in Fig. 6, relative to root canal filling volume, porosity volume, closed pore volume, and open pore volume. The Fig. 7 present the STL models of the five teeth submitted to the two scan modes.

Regarding the root canal filling volume (mm^3), in a single sampling scan mode, the volume for tooth 1 to 5, was 8.774, 7.200, 9.406, 12.446, 14.721, and in a multisampling scan mode was 8.617, 7.064, 9.444, 12.454, 14.721. The difference score for the single sampling scan mode and multisampling scan mode

regarding root canal filling volume was normally distributed, as assessed by the Shapiro-Wilk's test (p = 0.150). Data was reported as mean ± standard deviation. The root canal filling volume was lower when the multisampling scan mode was applied (10.460 ± 3.086 mm^3) as opposed to the single sampling scan mode (10.509 ± 3.028 mm^3). The multisampling scan mode elicited a decrease of 0.049 mm^3 (95 % CI, -0.063 to 0.161) in the root canal filling volume compared to the one achieved using the single sampling scan mode. However, this difference was not statistically significant (t (4) = 1.218, p = 0.290).

Regarding the porosity volume (mm^3), in a single sampling scan mode, the volume for tooth 1 to 5, was 0.064, 0.119, 0.263, 0.427, 0.391, and in a multisampling scan mode was 0.065, 0.123, 0.220, 0.391, 0.306. The difference score for the single sampling scan mode and multisampling scan mode regarding root canal filling volume was normally distributed, as assessed by the Shapiro-Wilk's test (p = 0.496). The porosity volume was lower when the multisampling scan mode was applied (0.221 ± 0.132 mm^3) as opposed to the single sampling scan mode (0.253 ± 0.161 mm^3). Regarding the porosity volume, the multisampling scan mode elicited a decrease of 0.032 mm^3 (95 % CI, -0.013 to 0.077) compared to the one achieved using the single sampling scan mode. However, this difference was not statistically significant (t (4) = 1.950, p = 0.123).

Regarding the closed pore volume (mm^3), in a single sampling scan mode, the volume for tooth 1 to 5, was 0.015, 0.007, 0.001, 0.026, 0.012, and in a multisampling scan mode was 0.018, 0.015, 0.001, 0.020, 0.011. The difference score for the single sampling scan mode and multisampling scan mode regarding root canal filling volume was normally distributed, as assessed by the Shapiro-Wilk's test (p = 0.865) The closed pore volume was 0.013 ± 0.007 mm^3 when the multisampling scan mode was applied as opposed to the single sampling scan mode (0.012 ± 0.009 mm^3). Regarding the closed pore volume, the difference between the multisampling and single sampling scan mode was 0.001 mm^3 (95 % CI, -0.007 to 0.006). This difference was not statistically significant (t (4) = -0.328, p = 0.760).

Regarding the open pore volume (mm^3), in a single sampling scan mode, the volume for tooth 1 to 5, was 0.049, 0.112, 0.262, 0.401, 0.379, and in a multisampling scan mode was 0.047, 0.108, 0.219, 0.371, 0.295. The difference score for the single sampling scan mode and multisampling scan mode regarding root canal filling volume was normally distributed, as assessed by the Shapiro-Wilk's test (p = 0.461). The open pore volume was lower when the multisampling scan mode was applied (0.208 ± 0.132 mm^3) as opposed to

the single sampling scan mode (0.241 ± 0.157 mm^3). Related to the open pore volume, the multisampling scan mode elicited a decrease of 0.032 mm^3 (95 % CI, -0.009 to 0.074) compared to the one achieved using the single sampling scan mode. However, this difference was not statistically significant (t (4) = 2.157, p = 0.097).

Overall, the results showed that the differences were not statistically significant. Although the standard deviation was high within the group itself, due to anatomical variability between the five analyzed teeth, the mean difference and standard deviation between the two groups (single and multi sampling scan mode) were very small. The difference between the two scan mode, regarding root canal filling volume, porosity volume, closed pore volume, and open pore volume was, respectively, 0.049, 0.032, 0.001, 0.032 mm^3. Considering the porosity, the difference between the two scan modes was more related to the differences of the open pore volume, as the closed pore volume was almost zero. These results are corroborated with some articles in the medical field, when a holder applied to *in vivo* positron emission tomography/computed tomography (PET/CT) scanning simultaneously small animals did not produce a significant loss of quantitative accuracy data, as well as considered the reduction of imaging cost (Cheng *et al.*, 2009; Habte *et al.*, 2013; Yagi *et al.*, 2014; Greenwood *et al.*, 2020).

3.3 Effect of single versus multisampling scan mode on the scan duration time, cost estimation, and data storage

The comparison of the scan duration time, imaging cost, and data storage, regarding the two scan modes, is shown in Table 3. In a single sampling scan mode, the total scan duration time to scan five teeth was 87 minutes and 42 seconds. In a multisampling scan mode, the scan duration time was 21 minutes and 51 seconds. Indeed, the reduction of the scan duration time constitutes an enormous advantage, and consequently, reduces human and equipment resources. Considering the effect of the scan mode on the scan duration time and on imaging cost, according to the settings selected in this work, the time and cost reduction with multisampling scan mode was 75 %. The definiton ‘scan time’ was strictly applied to compare the single to the multisampling scan mode. However, in a multisampling scan mode the ‘scan time’ could be complemented with the time used to separate, reconstruct and analyse the datasets generated. When the multisampling scan mode was adopted, the protocol followed by the authors implied that a single

reconstruction on NRecon software (Bruker SkyScan, Kontich, Belgium) was performed. Then, the five samples were separated into five datasets and aligned using Dataviewer software (Bruker SkyScan, Kontich, Belgium), and saved according to the respective number embossed on the holder. This separation could also be done latter on with CTAn software (Bruker SkyScan, Kontich, Belgium). However, the extra time for post-scan is less representative in comparison with the massive difference in the scan time.

In a multisampling scan mode, the required less data computer storage space was 6.9 GB contrasting with 17.1 GB for the five scans needed for a single sampling scan mode. The cost reduction with multisampling scan mode, considering the storage of data volume of all files created during the acquisition and reconstruction images, represented a reduction of 60 %.

The cost reduction also could be related to the preservation of the lifetime of the equipment, a reduction in human resources, a decrease in the time for post-acquisition data processing and analysis, and require less computer storage space.

4. Conclusion

The multisampling holder proposed herein provides the possibility to fit together, in a numbered position, several samples at the same time to do a multi-analysis by micro-CT. ABS plus™ P430 was the raw material selected to fabricate the holder allowing the higher percentage of X-ray transmission. Regarding the outcome, the results showed that comparing a single and multisampling scan mode the difference regarding the root canal filling volume, porosity volume, closed pore volume, and open pore volume was 0.049 mm^3, 0.032 mm^3, 0.001 mm^3, and 0.032 mm^3, respectively, which was not statistically significant. The multisampling scan mode estimated an enormous economic benefit, reducing time of scan and costs by 75 %, and data storage by 60 %. The small magnitude of differences between single and multisampling scan mode is a compelling result. There is a reduction no statistically significant different in porosity, both closed and open, in multisampling scan mode comparing with single sampling scan mode, even apply a sensitive indicator like porosity. The results both in the outcome parameter values and the quality of the images corroborate the use of the multisampling scan mode.

Declaration of Competing Interest

The authors declare that they have no known competing financial interests or personal relationships that could have appeared to influence the work reported in this paper.

Acknowledgements

This work was supported by the projects UID/Multi/04044/2013; UIDB/04044/2020; UIDP/04044/2020; PAMI - ROTEIRO/0328/2013 (No 022158) and UID/EMS/00481/2019-FCT - Fundação para a Ciência e a Tecnologia. This work was also supported by the projects UIDB/00481/2020 and UIDP/00481/2020 - FCT - Fundação para a Ciência e a Tecnologia; and CENTRO-01-0145-FEDER-022083 - Centro Portugal Regional Operational Programme (Centro2020), under the PORTUGAL 2020 Partnership Agreement, through the European Regional Development Fund.

The authors would like to thank Ruben da Silva for the technical support and to thank Luis Marques for the scientific support, both researchers associated with the Center for Rapid and Sustainable Product Development.

References

Alshehri M., Alamri H.M., Alshwaimi E., et al. Micro-computed tomographic assessment of quality of obturation in the apical third with continuous wave vertical compactation and single match taper sized cone obturation techniques. Scanning 2016;8:352-6. doi: 10.1002/sca.21277.

Angerame D., De Biasi M., Pecci R., et al. Analysis of single point and continuous wave of condensation root filling techniques by micro-computed tomography. Ann Ist Super Sanita 2012;48:35-41. doi: 10.4415/ANN_12_01_06.

ASTM F2792 -12 Standard Terminology for Additive Manufacturing Technologies, Standard. American Society for Testing Materials, West Conshohocken, USA (2012).

Boutsioukis C., Lambrianidis T., Verhaagen B., et al. The effect of needle-insertion depth on the irrigant flow in the root canal: evaluation using an unsteady computational fluid dynamics model. J Endod 2010;36:1664–8. doi: 10.1016/j.joen.2010.06.023.

Bouxsein M.L., Boyd S.K., Christiansen B.A., et al. Guidelines for assessment of bone microstructure in rodents using micro-computed tomography. Bone Miner Res 2010;25:1468–86. doi: 10.1002/jbmr.141.

Branco A.C., Silva R., Santos T., et al. Suitability of 3D printed pieces of nanocrystalline zirconia for dental applications. Dent Mater 2020;36:442–55. doi: 10.1016/j.dental.2020.01.006.

Celikten B., Uzuntas C.F., Orhan A.I., et al. Evaluation of root canal sealer filling quality using a single-cone technique in oval shaped canals: an in vitro micro-CT study. Scanning 2016;38:133–40. doi: 10.1002/sca.21249.

Cheng T.E., Yoder K.K., Normandin M.D., et al. A rat head holder for simultaneous scanning of two rats in small animal PET scanners: design, construction, feasibility testing and kinetic validation. J Neurosci Methods 2009;176:24–33. doi: 10.1016/j.jneumeth.2008.08.031.

Freire L.G., Iglecias E.F., Cunha R.S., et al. Micro-computed tomographic evaluation of hard tissue debris removal after different irrigation methods and its influence on the filling of curved canals. J Endod 2015;41:1660–66. doi: 10.1016/j.joen.2015.05.001.

Greenwood H.E., Nyitrai Z., Mocsai G., et al. High-throughput PET/CT imaging using a multiple-mouse imaging system. J Nucl Med 2020;61:292–7. doi: 10.2967/jnumed.119.228692.

Habte F., Ren G., Doyle T.C., et al. Impact of a multiple mice holder on quantitation of high-throughput microPET imaging with and without CT attenuation correction. Mol Imaging and Biol 2013;15:569–75. doi: 10.1007/s11307-012-0602-y.

Herrmann K-H., Gärtner C., Güllmar D., et al. 3D printing of MRI compatible components: why every MRI research group should have a low-budget 3D printer. Med Eng Phys 2014;36:1373–80. doi: 10.1016/j.medengphy.2014.06.008.

Iglecias E.F., Freire L.G., Candeiro G.T.M., et al. Presence of voids after continuous wave of condensation and single-cone obturation in mandibular molars: a micro-computed tomography analysis. J Endod 2017;43:638–42. doi: 10.1016/j.joen.2016.11.027.

Jiang L.M., Verhaagen B., Versluis M., et al. Evaluation of a sonic device designed to activate irrigant in the root canal. J Endod 2010;36:143–6. doi: 10.1016/j.joen.2009.06.009.

Ketcham R.A., Carlson W.D. Acquisition, optimization and interpretation of X-ray computed tomographic imagery: applications to the geosciences. Computers & Geosciences 2001;27:381–400. doi: 10.1016/S0098-3004(00)00116-3.

Khosravani M. R., Reinicke T. On the use of X-ray computed tomography in assessment of 3D-printed components. *Journal of Nondestructive Evaluation* 2020; 39:75. doi: 10.1007/s10921-020-00721-1.

Kim G.B., Lee S., Kim H., et al. Three-dimensional printing: basic principles and applications in medicine and radiology. Korean J Radiol 2016;17:182–97. doi: 10.3348/kjr.2016.17.2.182.

Latief F.D.E., Fauzi U., Irayani Z., et al. The effect of X-ray micro computed tomography image resolution on flow properties of porous rocks. J Microsc 2017, 266:69–88. doi: 10.1111/jmi.12521.

Leszczyński B., Gancarezyk A., Wróbel A., et al. Global and local thresholding methods applied to X-ray microtomographic analysis of metallic foams. J Nondestruct Eval 2016, 35:1–9. doi: 10.1007/s10921-016-0352-x.

Longo A.B., Sacco S.M., Salmon P.L., et al. Longitudinal use of micro-computed tomography does not alter microarchitecture of the proximal tibia in sham or ovariectomized sprague–dawley rats. Calcif Tissue Int 2016, 98:631–41. doi: 10.1007/s00223-016-0113-y.

Moeller L., Wenzel A., Wegge-Larsen A.M., et al. Quality of root fillings performed with two root filling techniques. An in vitro study using micro-CT. Acta Odontol Scand 2013;71:689–96. doi: 10.3109/00016357.2012.715192.

Moinzadeh A.T., Farack L., Wilde F., et al. Synchrotron-based phase contrast-enhanced micro-computed tomography reveals delaminations and material tearing in water-expandable root fillings ex vivo. J Endod 2016;42:776–81. doi: 10.1016/j.joen.2016.01.023.

van Noort R. The future of dental devices is digital. Dent Mater 2012;28:3–12. doi: 10.1016/j.dental.2011.10.014.

Ozdemir H.O., Buzoglu H.D., Calt S., et al. Chemical and ultramorphologic effects of ethylenediaminetetraacetic acid and sodium hypochlorite in young and old root canal dentin. J Endod 2012;38:204–8. doi: 10.1016/j.joen.2011.10.024.

du Plessis A., Broeckhoven C., Guelpa A., et al. Laboratory X-ray micro-computed tomography: a user guideline for biological samples. Gigascience 2017;6:1–11. doi: 10.1093/gigascience/gix027.

Rechenberg D.K., Paqué F. Impact of cross-sectional root canal shape on filled canal volume and remaining root filling material after retreatment. Int Endod J 2013;46:547–55. doi: 10.1111/iej.12027.

Sacco S. M., Saint C., Longo A.B., et al. Repeated irradiation from micro-computed tomography scanning at 2, 4 and 6 months of age does not induce damage to tibial bone microstructure in male and female CD-1 mice. BoneKey Rep 2017, 6:855. doi: 10.1038/bonekey.2016.87.

Siepel F.J., van Lier M.G.J.T.B., Chen M., et al. Scanning multiple mice in a small-animal PET scanner: influence on image quality. Nuclear Instruments and Methods in Physics Research, Section A 2010;621:605–10. doi: 10.1016/j.nima.2010.05.057.

van der Sluis L. W. M., Vogels M. P. J. M., Verhaagen B. et al. Study on the influence of refreshment/activation cycles and irrigants on mechanical cleaning efficiency during ultrasonic activation of the irrigant. J Endod 2010;36:737–40. doi: 10.1016/j.joen.2009.12.004.

van der Sluis L. W. M., Gambarini G., Wu M. K., Wesselink P. R. The influence of volume, type of irrigant and flushing method on removing artificially placed dentine debris from the apical root canal during passive ultrasonic irrigation. Int Endod 2006;472–76. doi: 10.1111/j.1365-2591.2006.01108.x.

Yagi, M., Arentsen L., Shanley R. M., Hui S. K. High-throughput multiple-mouse imaging with

micro-PET/CT for whole-skeleton assessment. Physica Medica 2014;30:849–53. doi: 10.1016/j.ejmp.2014.06.003.

Zhang D., Chen J., Lan G. *et al.* The root canal morphology in mandibular first premolars: a comparative evaluation of cone-beam computed tomography and micro-computed tomography. Clin Oral Investig 2017;21:1007–12. doi: 10.1007/s00784-016-1852-x.

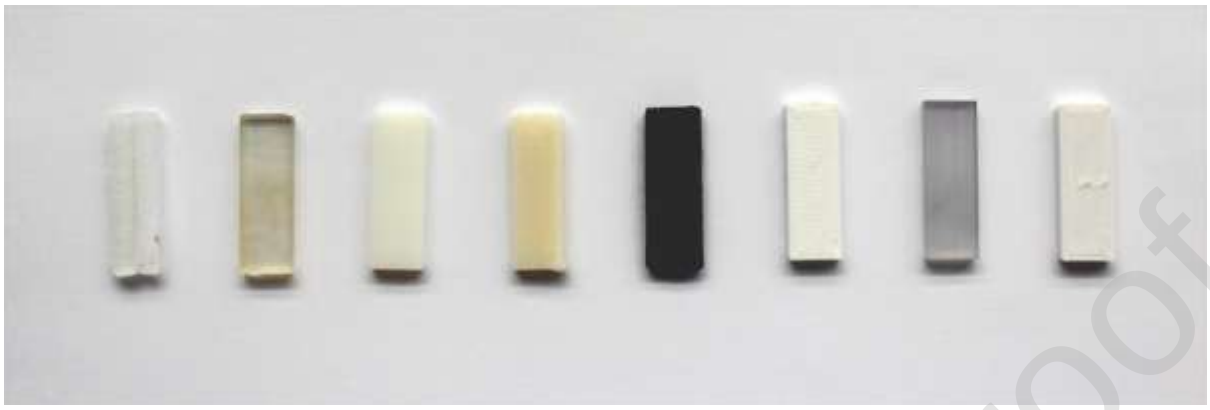

Figure 1. The eight raw materials tested to select the polymeric material for the 3D printed holder. From the left to the right: Dental Wax; RGD 720; Rigur™ RGD 450; ABSplus™ P430; ABS Black; PLA (Polylactic acid); VeroClear™; and PETG.

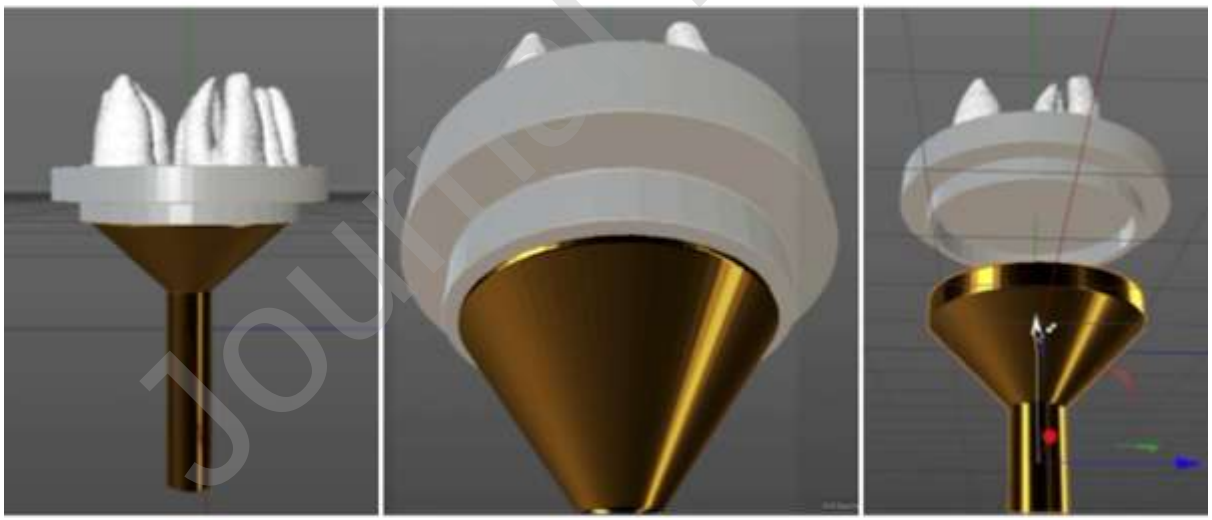

Figure 2. A micro-CT accessory supplied by Bruker SkyScan Micro-CT and a metallic brass tray sample, with a circular base of 25 mm in diameter and peripheral rim, was used to sustain the holder. The internal circular section externally fits the brass tray base supplied by the manufacturer, to stabilize the holder.

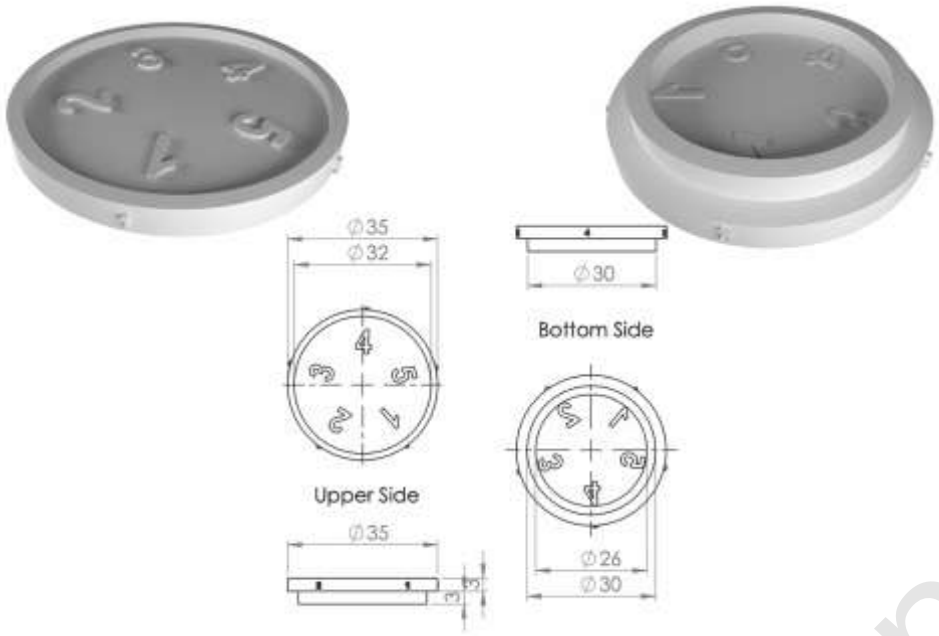

Figure 3. 3D model of the holder. Upper, side and bottom view dimensions of the holder design.

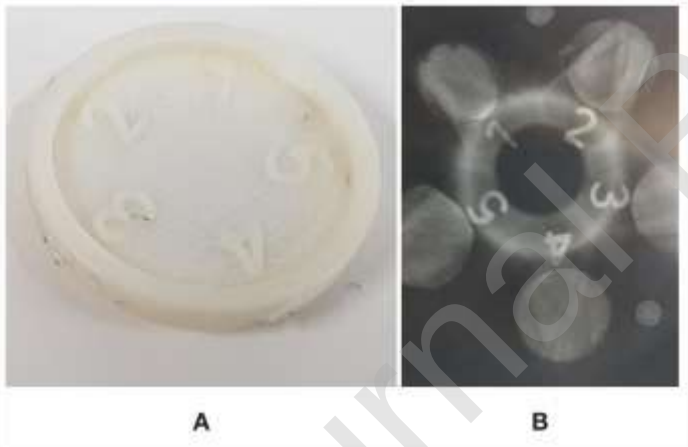

Figure 4. The numbers inserted in the holder **(A)** allow, after the scan, to identify and specify the samples **(B)**.

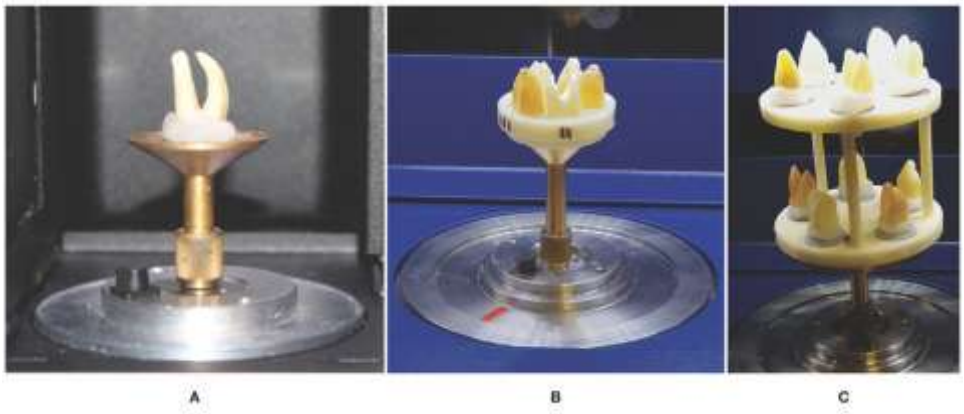

Figure 5. **A-** 'Traditional' way of sample mounting, using one sample per scan. **B-** Holder with the five teeth for a multisampling scan mode. **C-** Example of a holder with two platforms.

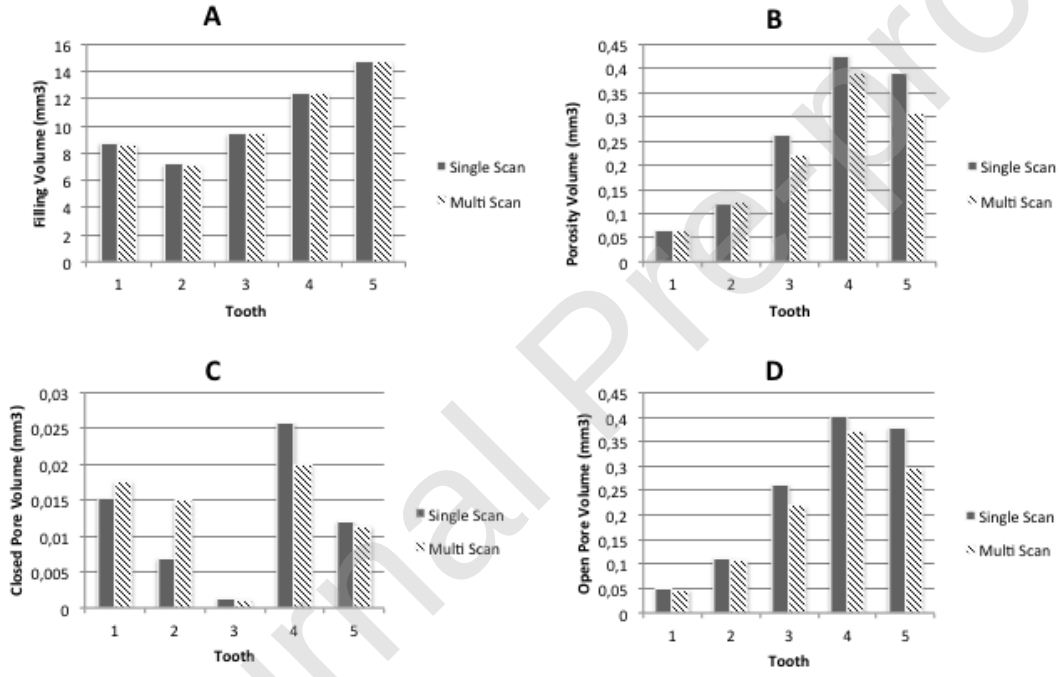

Figure 6. A- Root canal filling volume (mean ± standard deviation) (mm^3) **B**- Porosity filling volume (mean ± standard deviation) (mm^3) **C**- Closed pore volume (mean ± standard deviation) (mm^3) **D**- Open pore volume (mean ± standard deviation) (mm^3) comparing the single sampling scan mode and multi sampling scan mode.

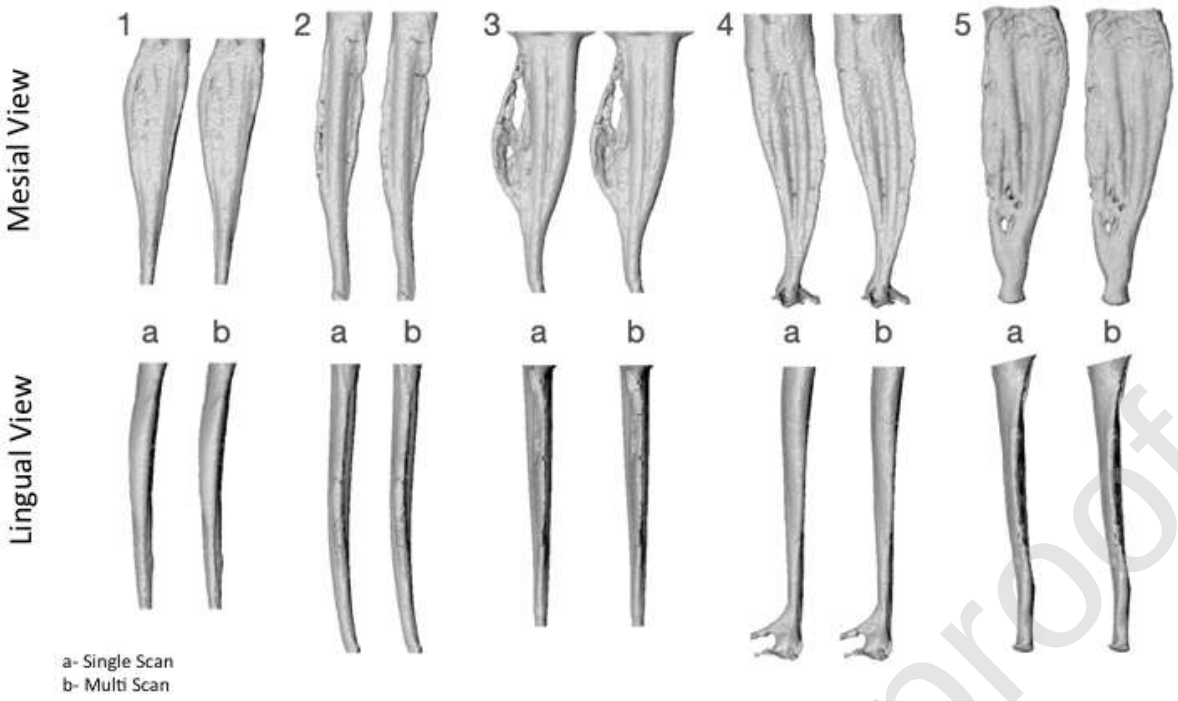

Figure 7. 3D models (mesial view and lingual view) from the five teeth obtained by the single and multisampling scan mode. a- Single sampling scan mode. b- Multi sampling scan mode.

Table 1. 3D-printer, slicer, raw material tested and commercial name, manufacturer and technology associated to the 3D printing process.

3D-Printer	Slicer	Raw Material	Material	Supplier	Technology
-	-	paraffin and hydrocarbon	Dental Wax	Kerr	-
Object 30Prime	Object Studio 9.2	arginylglycylaspartic acid	RGD 720	Stratasys	Material Jetting
Object 30Prime	Object Studio 9.2	arginylglycylaspartic acid	RGD 450	Stratasys	Material Jetting
Object 30Prime	Object Studio 9.2	polymethyl methacrylate	Vero Clear	Stratasys	Material Jetting
uPrint	GrabCAD Print 1.37	acrylonitrile butadiene styrene	ABS P430	Stratasys	Material Extrusion
BQ Hephestos 2	Ultimaker Cura 4.4	acrylonitrile butadiene styrene	ABS Black	Prima Value	Material Extrusion
BQ Hephestos 2	Ultimaker Cura 4.4	polylactic acid	PLA	BQ	Material Extrusion

BQ Hephestos 2	Ultimaker Cura 4.4	polyethene terephthalate glycol copolyester	PETG	RepRap	Material Extrusion

Table 2. Values of micro-CT transmission (%) through each raw material tested: Dental Wax; RGD 720; Rigur™ RGD 450 (RGD450); ABSplus™ P430; ABS Black; PLA; VeroClear™; PETG. Through the samples the assays were done in triplicate and showed as minimum (Min) of transmission and as average (Av), with and without flat-field (ff). The last row shows the average of the three assays (Avf), with ff correction.

	1 Dental Wax		**2 RGD 720**		**3 RGD 450**		**4 (ABS Plus)**		**5 (ABS black)**		**6 (PLA)**		**7 Vero clear**		**8 PET G**	
	Without ff	With ff	Without ff	With ff	Without ff	With ff	Without ff	With ff	Without ff	With ff	Without ff	With ff	Without ff	With ff	Without ff	With ff
ABOVE THE SAMPLE																
Min	56.5	87.1	55.5	86.0	56.1	86.3	54.5	87.1	56.1	86.7	56.1	87.5	57.3	87.5	55.3	86.9
Av	60.6	92.0	60.0	92.0	60.4	92.1	59.9	92.1	60.6	92.1	60.1	92.2	61.3	92.1	60.4	92.0
THROUGH THE SAMPLE																
Min	21.6	29.8	14.9	19.6	14.1	18.8	18.8	25.9	19.2	26.3	13.3	16.9	15.3	19.6	13.7	17.3
Av	55.6	83.7	54.9	82.3	53.9	81.7	55.2	84.3	56.1	84.5	54.5	81.7	54.9	81.9	53.8	81.2
Min	23.4	30.2	15.7	19.2	15.3	18.0	20.4	25.5	20.4	25.9	13.7	16.9	16.5	19.6	14.9	17.6
Av	58.3	83.7	58.6	81.9	57.3	81.6	59.3	84.4	59.6	84.1	57.7	81.6	57.9	81.7	57.1	81.0
Min	26.7	29.4	18.0	18.4	16.9	17.3	23.5	25.1	22.4	25.9	15.3	16.1	18.0	18.0	16.5	16.9
Av	67.5	83.7	68.0	82.1	66.3	81.7	69.0	84.3	67.2	84.1	65.3	81.5	66,6	81,7	66.0	81.1
Avf	-	83.7	-	82.1	-	81.7	-	84.3	-	84.2	-	81.6	-	81.8	-	81.1

Table 3. Estimated economic benefit of using a multisampling holder, considering five samples.

	Single_Scan	**Multi_Scan**	**Reduction**
Number of samples per scan	1	5	-
Number of scans	5	1	80 %
Time*	87:42	21:51	75 %
Cost**	4x	x	75 %
Storage***	17.1	6.9	60 %

* Time (minutes: seconds) of micro-CT scanning
** Scanning cost considering ‘x’ as a minor unit cost for micro-CT scanning
*** Data volume (GB) includes all files created during the acquisition image and reconstruction